Supporting Information

Revisiting π Backbonding: The Influence of *d* Orbitals on Metal-CO Bonds and Ligand Red Shifts

Daniel Koch,[a] Yingqian Chen,[a] Pavlo Golub[a] and Sergei Manzhos*[b]

Functional Test

In Table S1 the molar formation energies (see main text) of the $Mg(CO)_8$, $Ca(CO)_8$ and $[Ti(CO)_8]^{2+}$ complexes as well as the average change of the CO stretch frequencies in these complexes are listed for the M06 and B3LYP density functionals, a *cc*-pVQZ basis set and computational settings as described in the main text have been employed.

Table S1 CO stretch frequency changes (relative to free CO), and complex formation energies for $Mg(CO)_8$, $Ca(CO)_8$ and $[Ti(CO)_8]^{2+}$ complexes obtained with B3LYP/*cc*-pVQZ and M06/*cc*-pVQZ.

		$Mg(CO)_8$	**$Ca(CO)_8$**	**$[Ti(CO)_8]^{2+}$**
$\nu_0(CO)-\nu(CO)[cm^{-1}]$	B3LYP	-147	-130	+60
	M06	-136	-107	+61
E_f [kJ/mol]	B3LYP	-27	-298	-871
	M06	-110	-399	-998

[a] Department of Mechanical Engineering, National University of Singapore, 9 Engineering Drive 1, Singapore 117575

[b] Centre Énergie Matériaux Télécommunications, Institut National de la Recherche Scientifique, 1650, boulevard Lionel-Boulet, Varennes QC J3X1S2 Canada, Tel. : +1 514 2286841, Email: sergei.manzhos@emt.inrs.ca

Basis Set Test

In Figs. S1 and S2 the total energies and binding energies of the $Mg(CO)_8$ and $Ca(CO)_8$ complexes are shown with increasing size of the *cc*-pV*X*Z basis set (with *X*=D,T,Q,5), respectively.[1-4] As can be seen, energies are mostly converged form the triple-zeta level on. As a compromise between the additional accuracy the *cc*-pV5Z basis provides and computational feasibility, the *cc*-pVQZ basis set was chosen. Deviations between quadruple-zeta and quintuple-zeta level are less than 0.002 E_h (5.3 kJ/mol) towards stronger binding in both cases, which does not affect the conclusions drawn in the main text. The inclusion of more diffuse functions in form of an augmented *cc*-pVQZ basis set brought an additional gain in accuracy in the $Mg(CO)_8$ case, but since the aug-*cc*-pVQZ basis set is not available for Ca, and the results with *cc*-pVQZ on Ca and aug-*cc*-pVQZ on C and O are deviating more from the *cc*-pV5Z benchmark than with the *cc*-pVQZ basis on all atoms, no augmented basis sets were used.

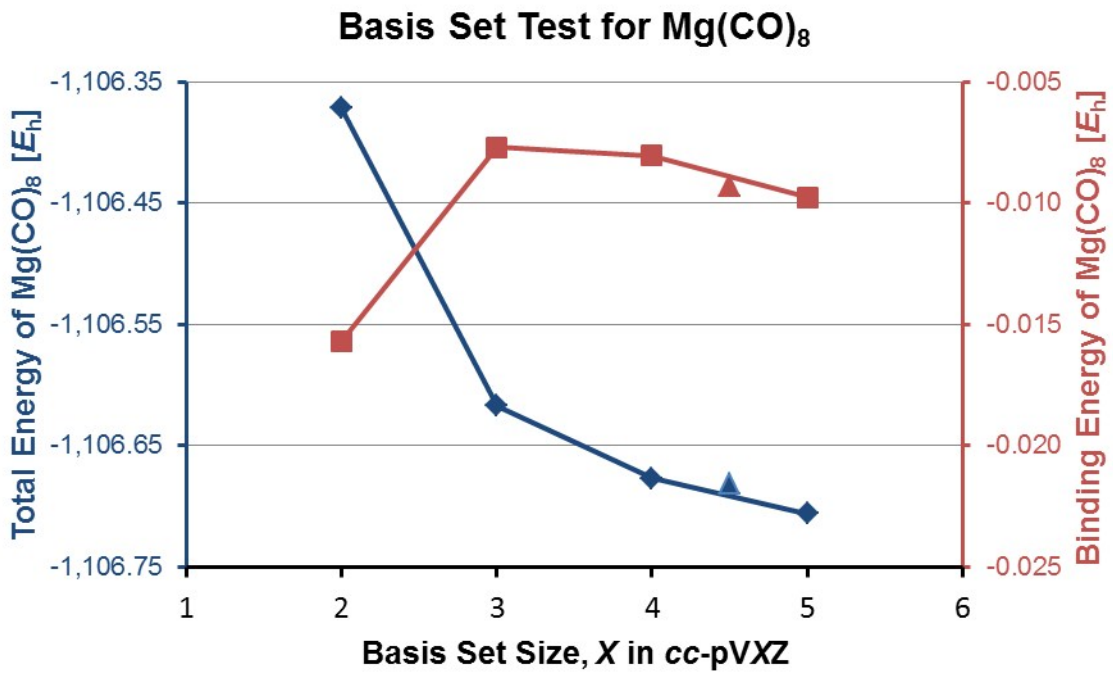

Fig. S1 Changes in total (blue, diamonds) and binding energy (red, squares) of the $Mg(CO)_8$ complex with increasing *cc*-pV*X*Z basis set size. *X* denotes the valence-zeta and varies between D (i.e. 2) and 5. The data point at *X*=4.5 (triangle) denotes values obtained with an aug-*cc*-pVQZ basis set for $Mg(CO)_8$ or *cc*-pVQZ on Ca/aug-*cc*-pVQZ on C and O for $Ca(CO)_8$ (since no corresponding augmented basis set for Ca is available).

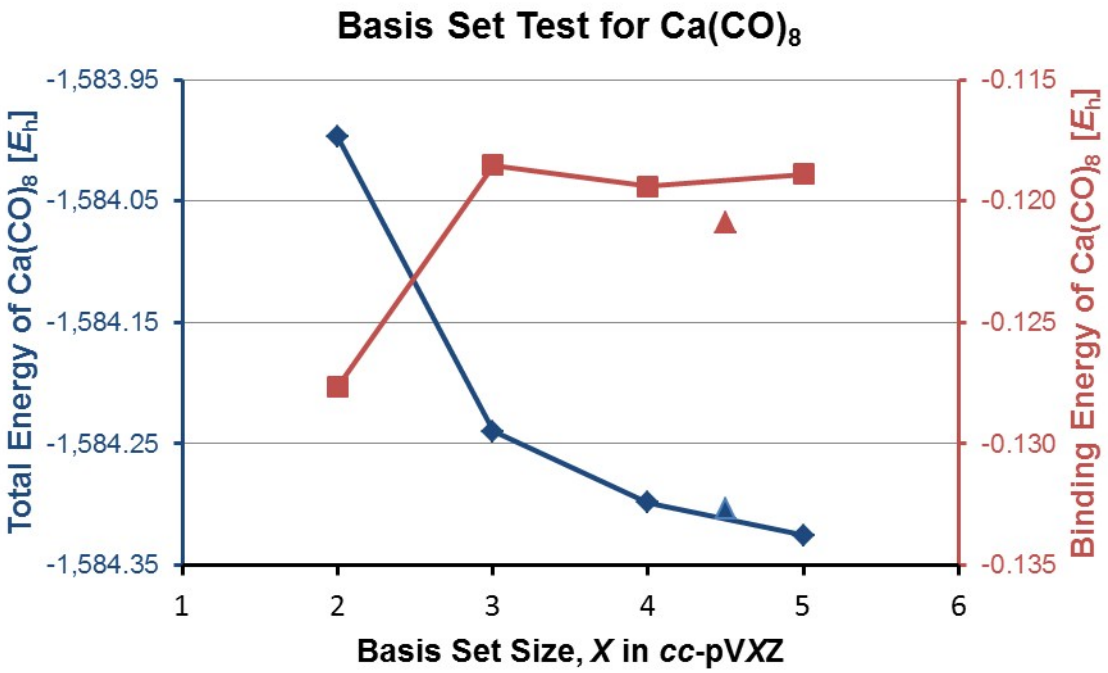

Fig. S2 Changes in total (blue, diamonds) and binding energy (red, squares) of the $Ca(CO)_8$ complex with increasing *cc*-pV*X*Z basis set size. *X* denotes the valence-zeta and varies between D (i.e. 2) and 5. The data point at *X*=4.5 (triangle) denotes values obtained with an *cc*-pVQZ on Ca/aug-*cc*-pVQZ on C and O for $Ca(CO)_8$ (since no corresponding augmented basis set for Ca is available).

In Fig. S3, the average CO stretch frequencies in $Mg(CO)_8$ and $Ca(CO)_8$ are shown with increasing size of the *cc*-pV*X*Z basis set (with *X*=D,T,Q,5). The average CO stretch frequencies converge quickly and deviate only within 1 cm^{-1} between *cc*-pVQZ and *cc*-pV5Z for these complexes, which is sufficiently precise for the conclusions drawn in the main text.

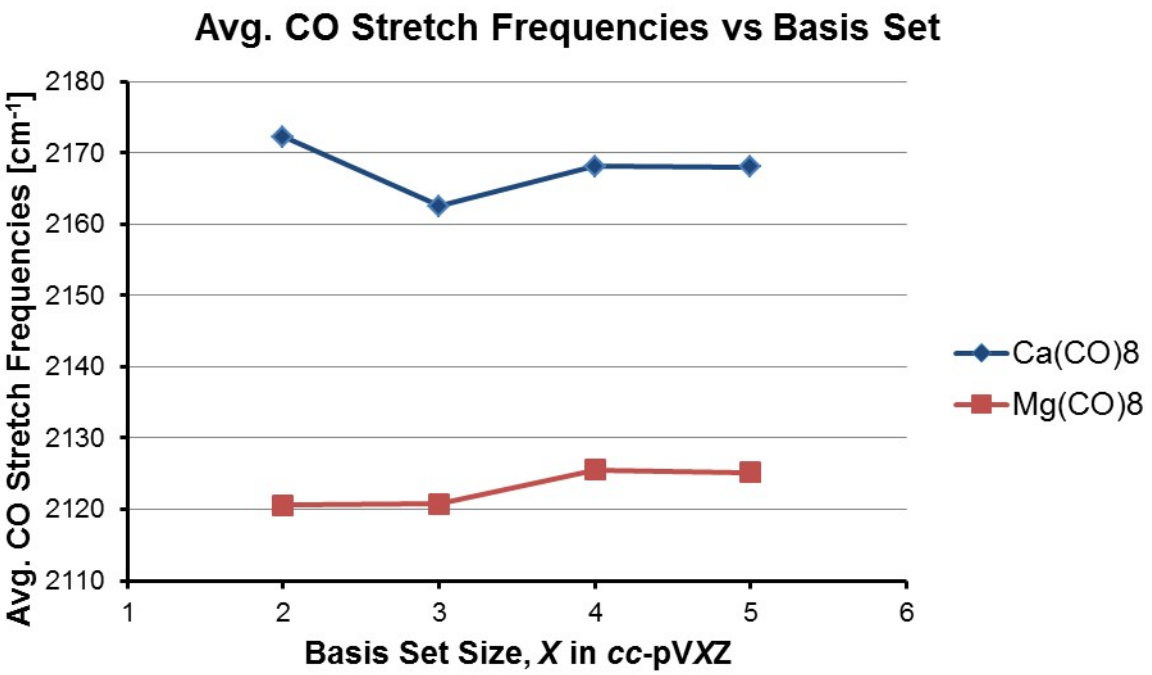

Fig. S3 Average CO stretch frequencies in the $Mg(CO)_8$ (red, squares) and $Ca(CO)_8$ (blue, diamonds) complexes with increasing *cc*-pV*X*Z basis set size. *X* denotes the valence-zeta and varies between D (i.e. 2) and 5.

Dispersive and Basis Set Superposition Error Effects

In Table S2 the total energy changes with an additional dispersion correction as proposed by Grimme *et al.* (DFT-D3)[5] for the three investigated complexes (with full *cc*-pVQZ basis and M06-2X functional[6] as implemented in the program package *Gaussian 16*[7]) are listed. Table S1 also includes the basis set superposition error[8, 9] for the three complexes with two fragments (Ca and $(CO)_8$), indicating the magnitude of overbinding introduced by mutual basis function borrowing. Both values are small in comparison to the binding energies of each complex (see main text).

Table S2 Dispersion correction with DFT-D3 and basis set superposition error (BSSE) for the three investigated complexes $Mg(CO)_8$, $Ca(CO)_8$ and $[Ti(CO)_8]^{2+}$ with M06-2X/*cc*-pVQZ.

Complex	***E*(DFT-D3)-*E*(DFT) [kJ/mol]**	**BSSE(Ca/$(CO)_8$) [kJ/mol]**
$Mg(CO)_8$	-2.23	3.28
$Ca(CO)_8$	-2.47	7.62
$[Ti(CO)_8]^{2+}$	-2.44	5.40

Influence of Complex Geometry

In Table S3 the Bader charges, CO red shifts, complex formation energies and delocalization indices for the electronically stable ^3O_h and $^1D_{4d}$ states of $Mg(CO)_8$ and $Ca(CO)_8$/$[Ti(CO)_8]^{2+}$, respectively, are listed as obtained at the M06-2X/*cc*-pVQZ level.

Table S3 Metal Bader charges, CO stretch frequency changes (relative to free CO), Complex formation energies and delocalization indices for $Mg(CO)_8$ (^3O_h), $Ca(CO)_8$ ($^1D_{4d}$) and $[Ti(CO)_8]^{2+}$ ($^1D_{4d}$) complexes obtained with M06-2X/*cc*-pVQZ.

	$Mg(CO)_8$ (^3O_h)	**$Ca(CO)_8$ ($^1D_{4d}$)**	**$[Ti(CO)_8]^{2+}$ ($^1D_{4d}$)**
q(M) [|*e*|]	+1.76	+1.44	+1.73
ν_0(CO)-ν(CO)[cm^{-1}]	-154	-112	+74
E_f [kJ/mol]	-21.1	-284.5	-894.1
DI(M-C)	0.035	0.082	0.158
DI(C-O)	0.815	0.826	0.868

Complex Geometries

In Tables S4 - S6, the optimized complex geometries for $Mg(CO)_8$, $Ca(CO)_8$ and $[Ti(CO)_8]^{2+}$ are listed in Cartesian coordinate representation as obtained with M06-2X/*cc*-pVQZ and convergence thresholds of 10^{-6} E_h for the total energy and $1.5 \cdot 10^{-5}$ E_h/a_0 for the interatomic forces.

Table S4 Optimized complex geometry in Cartesian coordinates of $Mg(CO)_8$ with M06-2X/*cc*-pVQZ and convergence thresholds of 10^{-6} E_h for the total energy and $1.5 \cdot 10^{-5}$ E_h/a_0 for the interatomic forces.

Atom	**Coordinates [Å]**		
	X	**Y**	**Z**
Mg	0.000000	0.000000	0.000000
C	0.000000	1.971875	1.317546
O	0.000000	2.664534	2.207685
C	-1.971875	0.000000	1.317546
O	-2.664534	0.000000	2.207685
C	1.971875	0.000000	1.317546
O	2.664534	0.000000	2.207685
C	-1.394326	-1.394326	-1.317546
O	-1.884110	-1.884110	-2.207685
C	1.394326	-1.394326	-1.317546
O	1.884110	-1.884110	-2.207685
C	1.394326	1.394326	-1.317546
O	1.884110	1.884110	-2.207685
C	0.000000	-1.971875	1.317546
O	0.000000	-2.664534	2.207685
C	-1.394326	1.394326	-1.317546
O	-1.884110	1.884110	-2.207685

Table S5 Optimized complex geometry in Cartesian coordinates of $Ca(CO)_8$ with M06-2X/*cc*-pVQZ and convergence thresholds of 10^{-6} E_h for the total energy and $1.5 \cdot 10^{-5}$ E_h/a_0 for the interatomic forces.

Atom	**Coordinates [Å]**		
	X	**Y**	**Z**
Ca	0.000000	0.000000	0.000000
C	1.501332	1.501332	1.501332
O	2.151550	2.151550	2.151550
C	1.501332	-1.501332	1.501332
O	2.151550	-2.151550	2.151550
C	1.501332	1.501332	-1.501332
O	2.151550	2.151550	-2.151550
C	-1.501332	-1.501332	-1.501332
O	-2.151550	-2.151550	-2.151550
C	-1.501332	1.501332	-1.501332
O	-2.151550	2.151550	-2.151550
C	-1.501332	1.501332	1.501332
O	-2.151550	2.151550	2.151550
C	1.501332	-1.501332	-1.501332
O	2.151550	-2.151550	-2.151550
C	-1.501332	-1.501332	1.501332
O	-2.151550	-2.151550	2.151550

Table S6 Optimized complex geometry in Cartesian coordinates of $[Ti(CO)_8]^{2+}$ with M06-2X/*cc*-pVQZ and convergence thresholds of 10^{-6} E_h for the total energy and $1.5 \cdot 10^{-5}$ E_h/a_0 for the interatomic forces.

Atom	**Coordinates [Å]**		
	X	**Y**	**Z**
Ti	0.000000	0.000000	0.000000
C	1.441580	1.441580	1.441580
O	2.082028	2.082028	2.082028
C	1.441580	-1.441580	1.441580
O	2.082028	-2.082028	2.082028
C	1.441580	1.441580	-1.441580
O	2.082028	2.082028	-2.082028
C	-1.441580	-1.441580	-1.441580
O	-2.082028	-2.082028	-2.082028
C	-1.441580	1.441580	-1.441580
O	-2.082028	2.082028	-2.082028
C	-1.441580	1.441580	1.441580
O	-2.082028	2.082028	2.082028
C	1.441580	-1.441580	-1.441580
O	2.082028	-2.082028	-2.082028
C	-1.441580	-1.441580	1.441580
O	-2.082028	-2.082028	2.082028

References

1. D. E. Woon and T. H. Dunning, *J. Chem. Phys.*, 1993, **98**, 1358-1371.
2. K. A. Peterson, D. E. Woon and T. H. Dunning, *J. Chem. Phys.*, 1994, **100**, 7410-7415.
3. R. A. Kendall, T. H. Dunning and R. J. Harrison, *J. Chem. Phys.*, 1992, **96**, 6796-6806.
4. T. H. Dunning, *J. Chem. Phys.*, 1989, **90**, 1007-1023.

5. S. Grimme, J. Antony, S. Ehrlich and H. Krieg, *J. Chem. Phys.*, 2010, **132**, 154104.
6. Y. Zhao and D. G. Truhlar, *Theor. Chem. Acc.*, 2008, **120**, 215-241.
7. M. J. Frisch, G. W. Trucks, H. B. Schlegel, G. E. Scuseria, M. A. Robb, J. R. Cheeseman, G. Scalmani, V. Barone, G. A. Petersson, H. Nakatsuji, X. Li, M. Caricato, A. V. Marenich, J. Bloino, B. G. Janesko, R. Gomperts, B. Mennucci, H. P. Hratchian, J. V. Ortiz, A. F. Izmaylov, J. L. Sonnenberg, Williams, F. Ding, F. Lipparini, F. Egidi, J. Goings, B. Peng, A. Petrone, T. Henderson, D. Ranasinghe, V. G. Zakrzewski, J. Gao, N. Rega, G. Zheng, W. Liang, M. Hada, M. Ehara, K. Toyota, R. Fukuda, J. Hasegawa, M. Ishida, T. Nakajima, Y. Honda, O. Kitao, H. Nakai, T. Vreven, K. Throssell, J. A. Montgomery Jr., J. E. Peralta, F. Ogliaro, M. J. Bearpark, J. J. Heyd, E. N. Brothers, K. N. Kudin, V. N. Staroverov, T. A. Keith, R. Kobayashi, J. Normand, K. Raghavachari, A. P. Rendell, J. C. Burant, S. S. Iyengar, J. Tomasi, M. Cossi, J. M. Millam, M. Klene, C. Adamo, R. Cammi, J. W. Ochterski, R. L. Martin, K. Morokuma, O. Farkas, J. B. Foresman and D. J. Fox, *Gaussian 16 Rev. B.01*, Wallingford, CT, 2016.
8. S. Simon, M. Duran and J. J. Dannenberg, *J. Chem. Phys.*, 1996, **105**, 11024-11031.
9. S. F. Boys and F. Bernardi, *Mol. Phys.*, 1970, **19**, 553-566.